International Journal of Oceans and Oceanography
ISSN 0973-2667 Volume 4, Number 1 (2010), pp. 17-28

http://www.ripublication.com/ijoo.htm

Sonic Layer Depth Variability in the Arabian Sea

T. V. S. Udaya Bhaskar[1], Debadatta Swain[2] and M. Ravichandran[3]

[1,3]INCOIS, Ministry of earth science, P.B. No. 21, IDA Jeedimetta, Hyedrabad, (AP) -500055, India
[1]E-mail: uday@incois.gov.in and [3]E-mail: ravi@incois.gov.in
[2]Space physic Laboratories, Dept. of space, VSSC, ISRO, Trivendrum, Karla-695022, India
[2]E-mail: d_swain@vssc.gov.in

Abstract

Spatial and temporal distribution of sonic layer depth (SLD) in the Arabian Sea (AS) was studied using temperature and salinity (T/S) profiles from Argo floats during the years 2003 – 2004 and World Ocean Atlas 2001 (WOA01) climatology. SLD was obtained from sound velocity profiles computed from T/S data. SLD variability as obtained from Argo matched well with those obtained from the WOA01 in certain locations and showed remarkable difference in some other. SLD variability in the AS is mainly related to seasonal variations in T/S owing to influence of seasonal phenomena as well as the geography of the region. Deeper SLDs were observed during summer monsoon (> 90 m) and winter monsoon (> 80 m) respectively. Up-welling and down-welling (Ekman dynamics) associated with the Findlater Jet controlled SLD during the summer monsoon. While in winter monsoon, cooling and convective mixing regulated SLD in the study region. Weak winds, high insolation and positive net heat flux lead to the formation of thin, warm and stratified sonic layer during pre and post summer monsoon periods, respectively. Examination of SLD in selected areas further revealed clear seasonal changes reflecting strong monsoon signals in the AS.

Keywords: Argo Float, Sonic Layer Depth, Arabian Sea, Sound, Wind Stress, Heat Flux.

Introduction

Acoustic system plays a very important role in many civilian and military applications. Ocean being almost opaque to electromagnetic radiation, sound is the

only means to probe the ocean interior. Speed of sound in ocean is one of the important oceanographic parameters that determine many of the characters of sound transmission in ocean. Ocean acoustic tomography is a tool for synoptic monitoring of large-scale oceanographic features [1]. Ocean properties such as currents and sub-surface parameters like temperature can be deduced by mapping the variations of sound speed in ocean [2]. A plot of sound speed (velocity), computed from temperature, salinity, and pressure values, as a function of depth is called the sound velocity profile (SVP).

Sonic Layer Depth (SLD), which can be obtained from the SVP, is the depth of maximum sound speed above the deep sound channel axis. The deep sound channel, also known as the SOFAR is a subsurface duct for long-range transmission of acoustic signals where the sound rays are alternatively refracted and reflected. The surface duct is a zone bounded by the sea surface and SLD. The surface duct is the acoustical equivalent of oceanographic mixed layer depth (MLD). Mixed layer is a quasi-isothermal layer of water created by wind-wave action and thermohaline convection. While SLD is normally defined in terms of the sound-speed gradient, MLD is defined in terms of density (which is function of temperature, salinity and pressure) [3][4]. Depth of mixed layer is often used as an input variable in algorithms used for prediction of surface duct propagation. The near-surface maximum value of sound speed is usually located at the SLD [5] and a submerged object goes undetected by surface sonar at a depth of SLD plus 100 m and beyond (http://www.fas.org/man/dod-101/sys/ship/deep.htm). In general in normal three-layered ocean, SLD is frequently at the same depth as the MLD. However SLD and MLD are not always same because sound speed is substantially more sensitive to temperature than to salinity compared to density [6]. Though temperature is the primary controller of sound speed, the effect of pressure on sound speed is a function of depth. The effect of salinity on sound speed is slight in the open ocean, because salinity values are pretty much constant. However, the effect of salinity is greatest where there is a significant influx of fresh water or where surface evaporation creates high saline waters. Figure 1 presents a typical example of vertical profiles of temperature, salinity, and sound speed along with SLD in the Arabian Sea (AS).

Until recently, SVP was being obtained using XBT (Expendable Bathy-Thermograph) temperature profiles data, without considering the salinity contributions. In spite of little effect on sound speed, the need to obtain accurate SLD makes it essential to consider the contribution of salinity, while computing sound velocity, and thus SVP. In this context, climatological temperature and salinity (T/S) data sets can be used to study the SLD variability. However, operational monitoring of SLD variability accurately makes it necessary to have T/S data sets on a near real time basis. Such a requirement has been fulfilled to a larger extent by the deployment of Argo floats under the international Argo project that began in the year 2000. These profiling floats have enormous application capabilities in terms of providing real-time T/S profiles within the upper 2000 m of the ocean. The data obtained from these floats could be used to describe the seasonal cycle and interannual variability of the upper ocean thermo-haline circulation [7][8].

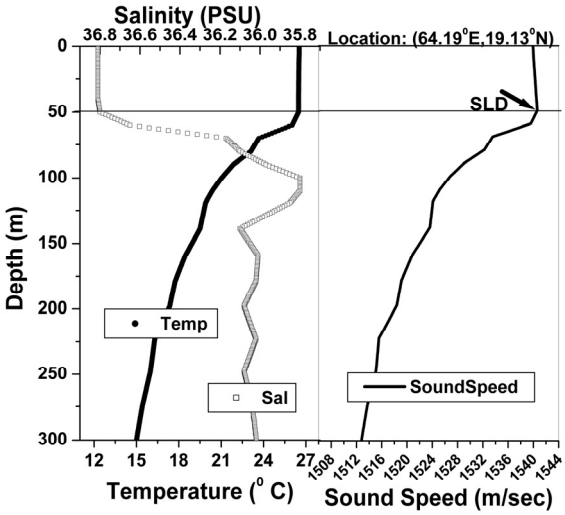

Figure 1: Typical vertical profiles of temperature, salinity, and sound speed along with SLD in the Arabian Sea (location: 19.13 ºN, 64.19 ºE).

In the present analysis, we obtain SLD using Argo floats T/S data in the AS region, extending from 30º E to 80º E and 0º to 30º N during January 2003 to December 2004. We have also used World Ocean Atlas 2001 (WOA01) [9] data to have a comparison between Argo and climatology. We then studied the SLD distribution and its variability during the same period. The AS is unique in that it is limited in the north by the Asian sub-continent. One consequence of this geography is that the AS is forced by intense, annually reversing monsoon winds. [10] have attributed maximum spatial variation in sound speed in this region to the combined effect of variations in T/S. Therefore, significant inference and insights about the seasonal variability of SLD can be obtained for the AS from a comprehensive study utilizing Argo data. However, so far very few studies on sound velocity and its variability in the AS regions have been carried out using limited data sets, only a significant one being that by [10]. They have attempted to study the sound speed structure in this region with annual mean climatological T/S data of Levitus [11]. But, no studies on SLD variability in the AS have been taken up so far. We believe that our work will be a useful contribution in understanding the regional and seasonal variability of SLD in AS.

Data and Methodology

Argo floats' T/S data in the study region from January 2003 to December 2004 were obtained from the Indian National Centre for Ocean Information Services (INCOIS) website (http://www.incois.gov.in/Incois/argo/argo_webGIS_intro.jsp#). This is made available by United States Global Ocean Data Assimilation Experiment (USGODAE) and Institut français de recherche pour l'exploitation de la mer (IFREMER). These floats measure T/S from surface to about 2000 m depth every 5/10 days. About 4212

T/S profiles were available from January 2003 – December 2004 in the study area. The data obtained were subjected to quality control checks [12], and the profiles that did not pass these checks were excluded from the study. The density distribution of the profiles in the study region that were used in the final analysis is shown in Figure 2.

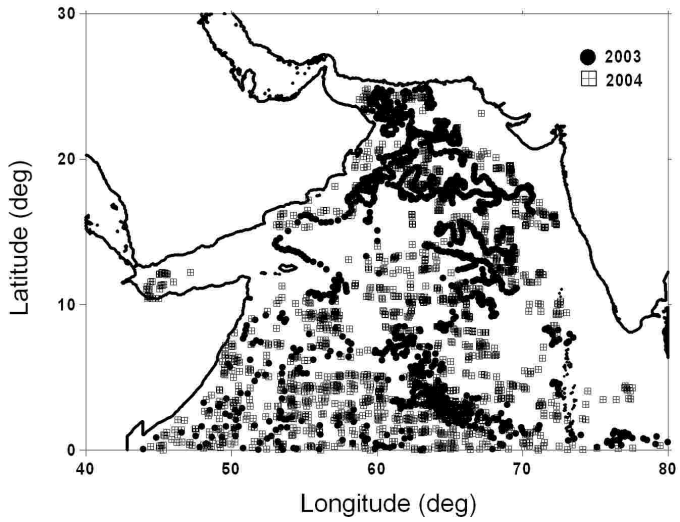

Figure 2: Location map of Argo profiles in the study region for the period January 2003 – December 2004.

Since data is unavailable at regular depths for all the floats, we uniformly interpolated the profiles linearly to 1 m depth resolution until 1000 m for all the observations. These T/S data sets were then used to compute sound speed at each depth following [13]. SLD was then estimated from these SVP as the depth of near surface maximum sound speed [5]. For this, the vertical sound speed gradient is checked at each depth resolution starting from the ocean surface. The depth below which, the sound speed gradient undergoes a change in sign is considered as the SLD. For WOA01, SLD was computed directly from the available 1º X 1º grided T/S data at the corresponding Argo float locations. Henceforth, we refer SLD obtained from Argo T/S data as SLD_A and that using WOA01 data as SLD_W. The individual SLD values for each month were then averaged to obtain monthly average SLDs. SLD anomalies were computed for each of the months for both 2003 and 2004 as SLD_A - SLD_W. The present work aims at studying the SLD variability as inferred from the T/S measured by Argo floats. Further, we intend to observe the spatial and the seasonal variability of SLD in the AS employing these data.

Results and Discussion

Sound speed being primarily controlled by temperature, salinity, and pressure, varies with the seasonal variations in T/S. Further, T/S being functions of geographical location, SVP is also dependent on it. Spatial variations of sound speed cause acoustic rays to bend according to Snell's law [14]. Regions of strong currents being associated with strong fronts in ocean T/S, act strongly to refract sound waves thus contributing to SLD variability. The influence of seasons on SLD variability is studied and a detailed analysis is presented in the following sub-sections.

Spatial distribution of SLD

During the northeast monsoon (December, January, February), the effect of wind forcing is weak compared to southwest monsoon and convective mixing due to winter cooling plays a significant role in varying the sound speed. Convective mixing causes the cool surface waters to sink into the deeper layers, thus mixing the temperature uniformly up to the mixed layer region. The associated temperature changes result in deepening of SLD in the entire AS. Consequently, during the northeast monsoon season (Figure 3a), SLD_A developed fairly deep and the floats in the northern AS recorded SLD_A values exceeding 80 m at certain locations. Large values of SLD_A were also observed in the interior AS. This region is influenced by Ekman convergence associated with strong negative wind stress curl, which tends to move water from southeast to northeast of the wind axis [15]. A band of minimum SLD_A was observed in the vicinity of equator for both the years. SLD_A was found to increase gradually from the equator towards northern AS, recording a maximum value of 99 m (88 m) in the month of January during this season for 2003 (2004) as compared to maximum SLD_W values of 71 m in January in this region. Though, areas of large SLD_A generally correspond to the regions of large SLD_W, significant differences were observed between SLD_A and SLD_W values in many regions of the AS (Figure 3c). SLD_A was systematically deeper by ~40 m than SLD_W south of 8° N and deeper than SLD_W by ~70 m in the northern AS for both the years.

The pre-monsoon months (March, April, and May) are marked with rise in solar insolation but reduced wind activity [16][4]. As a consequence, the north Indian Ocean warms up. This brings in a wide variation in SLD in the AS. During this season, SLD_A shallowed significantly in the northern AS (Figure 3b). Increase in solar insolation causes the surface layer to get heated up faster to relatively higher temperatures compared to the bottom layer thus resulting in shallower SLD. On the contrary, deeper SLD_A values of 49 (40) m were observed at certain locations in the southern AS (between 0° - 6° N) for 2003 (2004). These regions are also the regions of higher SLD anomalies (Figure 3d). SLD_A was found to be deeper by ~20 to 30 m than SLD_W through out the AS. The high SLD_A and high anomalies close to the equator can be associated with the presence of southward Somali undercurrent that developed during March, and is subsequently forced remotely by Rossby waves [16][17].

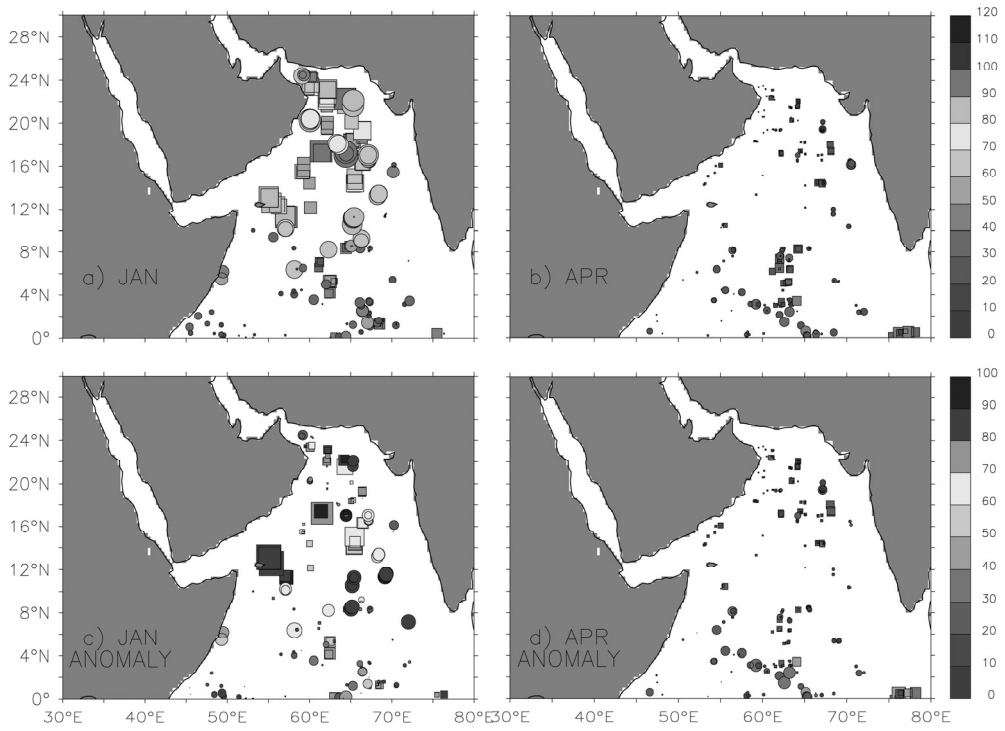

Figure 3: Horizontal distribution of SLDs for the months representative of the seasons: (a) Northeast monsoon (January), (b) Pre-monsoon (April); (c) January Anomaly, and (d) April Anomaly. Warmer/colder colors as well as larger/smaller areas indicate deeper/shallower SLDs. For anomalies larger/smaller areas as well as warmer/colder colors indicate SLD_A is larger/smaller than SLD_W respectively. Squares and circles (centred at the profile location) are representative of the years 2003 and 2004.

The summer monsoon season (June, July, August, and September) is marked by high wind activity and reduction in solar insolation due to cloud cover. SLD developed fairly deep in the central AS and SLD_A exceeding 90 m were often observed (Figure 4a). Owing to the influence of strong monsoon winds, there is strong down-welling in the central AS and up-welling in the northern AS [18]. The effect of this phenomenon is clearly seen from Figure 4a, with deeper SLD_A in the central AS and a decreasing trend towards the south and coastal regions. A maximum SLD_A of 101 (119) m was observed during 2003 (2004). SLD_A were systematically deeper by 30 m than SLD_W to the north of 16° N, whereas in the central AS, SLD_A was deeper than SLD_W by ~70 m or higher (Figure 4c) for both the years. SLD developed fairly deep during this season compared to all the four seasons.

The post-monsoon season (October, November) is characterized by the withdrawal of the southwest monsoons. The winds becomes westerlies, north of equator along 60° E to 90° E, with a strong eastward current along the equator, the Wyrtki jet [19]. During this season, relatively high SLD values as compared to other

regions are observed at float locations close to the equator, which is a contribution of this eastward current. However, overall SLD is shallower compared to the monsoon seasons (Figure 4b). SLD anomalies were also found to be large in this region for both the years (Figure 4d). Overall SLD_A is systematically deeper than SLD_W by ~20 m to 30 m for both 2003 and 2004. Further, both the SLD estimates, SLD_W and SLD_A are observed to be shallower to the north of 10° N with deeper SLD values in the eastern part. This can be attributed to the piling up of water towards the east as a result of the prevailing westerlies, resulting in downward sloping from west to east [20].

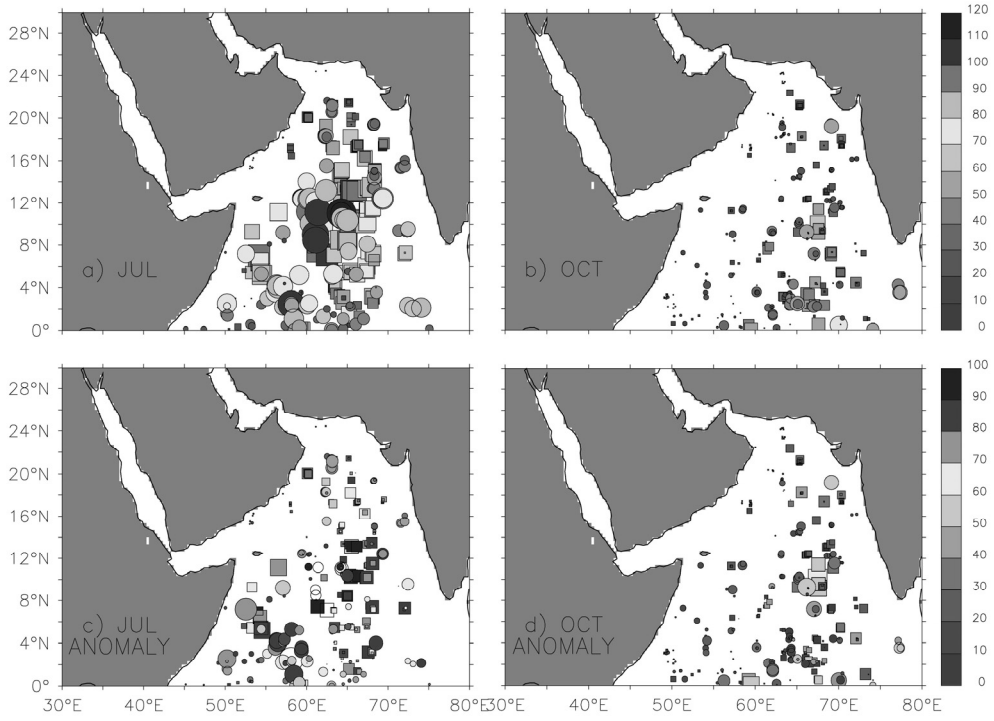

Figure 4: Same as Figure 3, except for the months representative of the seasons: (a) Southwest monsoon (July), (b) Post-monsoon (October); (c) July Anomaly, and (d) October Anomaly.

Year-to-Year variability of SLD in selected areas

In order to study the seasonal evolution and year-to-year variability of the sonic layer in detail, three small regions were selected representing the northern AS (NAS) [20° N – 25° N and 62° E – 67° E], central AS (CAS) [10° N – 15° N and 62° E – 67° E] and southern AS (SAS) [0° N – 5° N and 62° E – 67° E]. The grid size of 5° X 5° was selected considering the spatial resolution of Argo float array. The cumulative number of float observations used to study the temporal change of sonic layer was 212 in NAS, 207 in CAS and 354 in SAS regions for at least two seasons, during the analysis period of two years. Average maximum SLDs and months of their occurrence (within

braces) both from Argo floats and WOA01 for the three selected regions are presented in Table1. We also analysed wind stress from QuikScat [ftp.ifremer.fr/ifremer/cersat/products/gridded/mwf-quikscat/data] and surface heat flux from NCEP/NCAR reanalysis data [http://www.cdc.noaa.gov] in relation to SLD_A variability in the three regions during the study period.

The year-to-year variability of monthly averages of SLDs in the three regions is presented in Figure 5. Two cycles of seasonal variations are observed in all the three regions. A look at Figure 5 reveals significant year-to-year variability in all the three regions. Infact, large differences are observed for some of the months during the study period. A comparison of SLD_A and SLD_W further revealed notable differences in SLD values as well as months of occurrence of maxima and minima. The correlation coefficient (R) between SLD_A and SLD_W is observed to be 0.61, 0.89 and 0.67 for NAS, CAS and SAS respectively. In NAS, maximum SLD_A values of 68 m (49 m) were observed in the month of December for 2003 (2004), with the difference between two annual maxima being 19 m. SLD_W of 40 m was observed in the month of January (Table 1). Convection plays a major role in mixing the surface layers during winter [16]. Based on NCEP/NCAR reanalysis data, the monthly mean heat gain in this region in December 2004 was found to be 128 Wm^{-2} as against 150 Wm^{-2} in December 2003 (Figure 6a, 6b). Thus, deeper SLD in 2003 as compared to 2004 is a result of more heat gain that resulted in heating the surface layer by convective mixing.

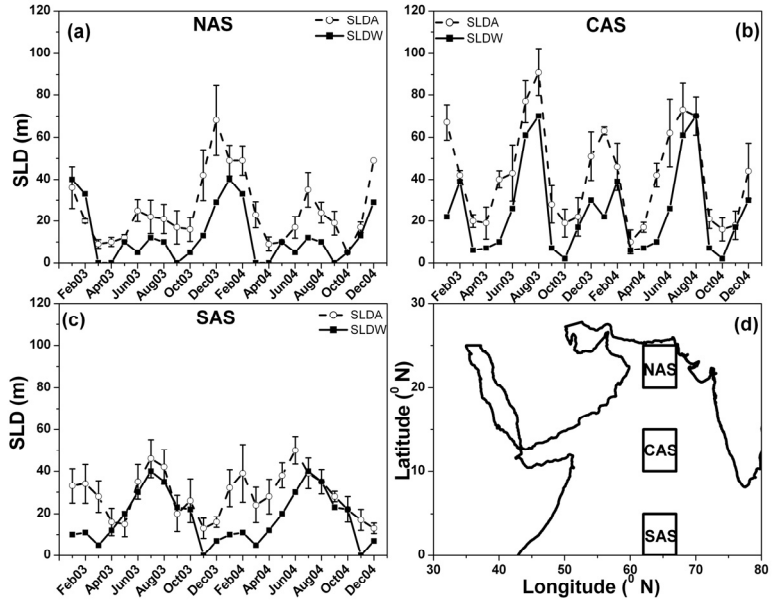

Figure 5: Year- to-year variability of SLD in selected areas: (a) Northern Arabian Sea (NAS), (b) Central Arabian Sea (CAS), (c) Southern Arabian Sea (SAS), and (d) Map of the regions selected. The values presented are monthly mean spatial averages.

In CAS, maximum SLD_A value of 91 m (73 m) were observed in the months of August (July) for 2003 (2004), with the difference between the two annual maxima being 18 m (Table 1). In case of SLD_W, maximum of 70 m was observed during August. Large deviations between SLD_W and SLD_A were observed during the post monsoon season in 2003 and during the pre-monsoon period of 2004 (Figure 5b). It is know that wind stress plays a major role in mixing the surface layer in this region during the summer monsoon period. Based on QuikScat observations maximum monthly mean wind stress value of 0.285 Nm^{-2} was obtained in August 2003 as compared to 0.269 Nm^{-2} in July 2004(Figure 6c, 6d). The analysis revealed the role of wind stress in SLD variability suggesting, deeper SLD in 2003 compared to 2004 could be a result of high wind stress that resulted in mixing surface layer hence deepening SLD_A.

Role of wind stress and surface fluxes is not as strong as it is in NAS and CAS as revealed from figure (figure 6e, 6f). In SAS (Figure 5c), the maximum SLD_A was observed to be 46 (50) m in month of July (June) for 2003 (2004) (Table 1). Maximum SLD_W of 40 m was observed in the month of July. Maximum SLD_A for the year 2004 occurred one month later as compared to SLD_W, while they occurred during the same months in 2003.

Analysing the four seasons (mentioned above) clearly revealed that seasonal variation of SLD coincided with the seasonal variations in net heat flux and winds. High correlation was observed between SLD-net heat flux and SLD-wind speed. While SLD had negative correlation with net heat flux, it had positive correlation with wind. This high correlation is a reflection of the similarity in seasonal variations of the two observations.

Table 1: Maxima and minima SLD_A, SLD_W, and anomalies for the selected areas, NAS, CAS, and SAS for 2003 and 2004 along with the months of occurrence mentioned in braces. (Note: The values presented are the values obtained in the selected regions, and neither temporal nor spatial averages).

REGION	YEAR	SLD_A (m)		SLD_W (m)	
		Maximum	Minimum	Maximum	Minimum
NAS	2003	68 (Dec)	9 (Mar)	40 (Jan)	0 (Apr)
	2004	49 (Dec)	5 (Oct)		
CAS	2003	91 (Aug)	19 (Apr)	70 (Aug)	2 (Oct)
	2004	73 (Jul)	10 (Mar)		
SAS	2003	46 (Jul)	13 (Nov)	40 (Jul)	0 (Nov)
	2004	50 (Jun)	13 (Dec)		

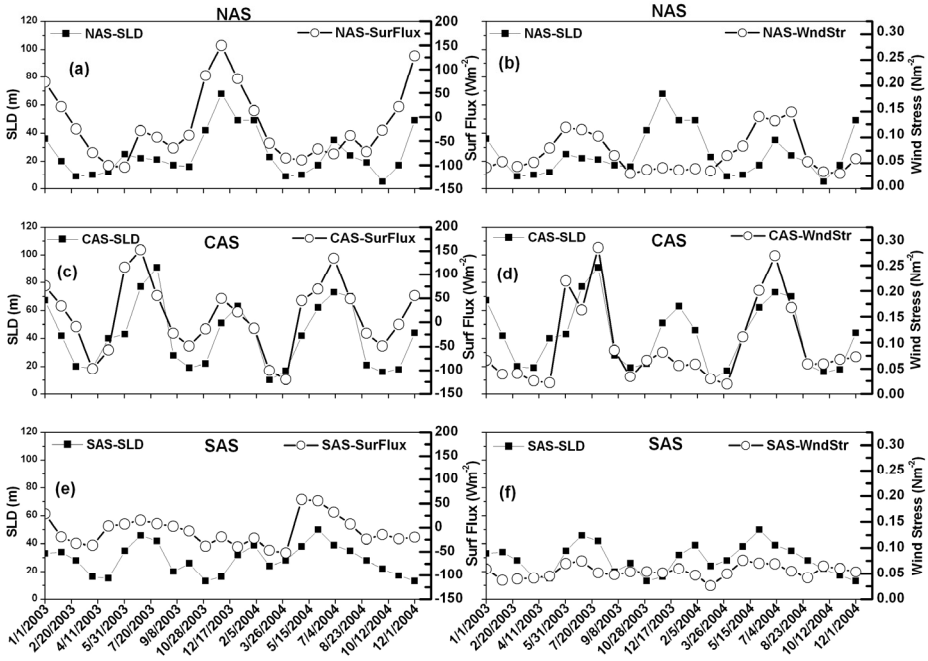

Figure 6: Variability of SLD with Wind Stress and Surface Fluxes: (a)&(b) Northern Arabian Sea (NAS), (c)&(d) Central Arabian Sea (CAS), (e)&(f) Southern Arabian Sea (SAS)

Summary and conclusions

In the present work we attempted to study the spatial and temporal variability of SLD in the AS using Argo floats' T/S data. This region being unique in its geographic location is influenced by various seasonal oceanographic and atmospheric circulation phenomena. The reversing monsoon winds are particularly interesting and we have studied the effect of such seasonal phenomena and regional location on SLD variability in the AS. We have also used WOA01 climatology data to have a comparison of SLD estimated using Argo profiles.

Variations in SLD in the AS are primarily a consequence of the seasonal variations in T/S and the geography of the region. Up-welling and transport variations in the AS result in spatial and seasonal variations of sound speed, and in turn result in variations of SLD. Both coastal and open-ocean up-wellings, particularly during the northeast and southwest monsoons, play a major role in SLD variability. Ekman convergence in the central AS together with coastal up-welling along the coasts of Somalia, Arabia and northern most corners of the AS are responsible for deeper SLD in the central AS and relatively shallow SLD along the coasts during the southwest monsoon. The monsoon winds contribute dominantly to SLD variability. SLD variability during the northeast monsoon is largely because of convective mixing due to winter cooling. Shallow SLD in the study region during the pre and post monsoon

months are due to the absence of wind action and are largely on account of the coastal currents and radiation forcing by Rossby waves from the west coast of India.

SLD_A are confined to about 90 m in the AS with high SLD values obtained during the southwest monsoons. Whereas, SLD_W values are much lower with maximum SLD of ~70 m and the lowest values being 0 m. The large difference in SLD can be attributed to smoothening of T/S profiles in WOA01 climatology. Strong seasonal signals are reflected in SLD variability with maximum spatial variability observed during the monsoon periods. Large SLD variability is also observed in the central AS compared to the coastal regions. Comparison of SLD_A with SLD_W reveals that climatology alone is not sufficient for real-time/operational monitoring of SLD in the AS. It is of significance to improve existing climatologies by incorporating valuable real-time *in situ* data sets like that from Argo. Assimilation of Argo data along with climatology would also contribute in improving existing ocean general circulation and coupled ocean-atmosphere models.

Acknowledgements

The authors thank the Director, Indian National Centre for Ocean Information Services (INCOIS) for his encouragement. Argo data were collected and made freely available by the International Argo Project and the national programmes that contribute to it (http://www.argo.ucsd.edu, http://argo.jcommops.org). The authors wish to acknowledge the use of Ferret, a product of NOAA's Pacific Marine Environmental Laboratory, for analysis and graphics in this paper.

References

[1] Munk, W. H., and Wunsch, C., 1979, "Ocean acoustic tomography: a scheme for large scale monitoring," Deep Sea Research. *A*, **26**, pp. 123 – 161.

[2] Spiesberger, J. L., Frye, D. E., O' Brien, J., Hurlburt, H., McCaffrey, J. W., Johnson, M., and Kenny, J., "Global acoustic mapping of Ocean temperatures (GAMOT)," proceedings of IEEE – Oceans, pp. 253 – 257.

[3] Kara, A. B., Rochford, P. A., and Hurlburt, H. E., 2003, "Mixed layer depth variability over the global ocean," Journal of Geophysical Research., *108 (C3)*, 3079.

[4] Udaya Bhaskar, T.V.S., Swain, D., and Ravichandran, M., 2006, "Inferring mixed-layer depth variability from Argo observation in the western Indian Ocean," Journal of Marine Research, 64, pp. 393-406.

[5] Etter, C. P., 1996, Underwater Acoustic Modelling: Principles, Techniques and Applications. 2nd ed., E & FN Spon, London.

[6] Helber, R.W., Barron, C.N., Carnes, M.R., and Zingarelli, R.A., 2008, "Evaluating the sonic layer depth relative to the mixed layer depth," Journal of Geophysical Research., 113, C07033.

[7] Argo Science Team., 2001, "The Global Array of Profiling Floats, in *Observing Oceans in the 21st Century*", C. Z. Koblinsky and N. R. Smith, eds., Godae Proj. Off., Bur. Meteorol., Melbourne, Australia, pp. 248 – 258.

[8] Ravichandran, M., Vinaychandran, P. N., Joseph, S., and Radhakrishnan, K., "Results from the first Argo float deployed by India," Current Science, **86**, pp. 651 – 659.

[9] Conkright, M. E., Locarnini, R. A., Garcia, H. E., O`Brien, T. D., Boyer, T. P., Stephens, C., and Antonov, J. I., 2002, *"World Ocean Atlas 2001: Objective Analysis, Data Statistics, and Figures"*, [CD-ROM] Natl. Oceanogr. Data Cent., Silver Spring, Md.

[10] Prasanna Kumar, S., Navelkar, G. S., Ramana Murty, T. V., Somayajulu, Y. K., and Murty, C. S.,"Sound speed structure in the Arabian Sea and the Bay of Bengal," Indian Journal of Marine Sciences, **22**, pp. 17 – 20.

[11] Levitus, S.,1988, "Climatological Atlas of the world ocean," *NOAA professional paper 13*, US Government Printing Office, Washington DC.

[12] Wong, A., Keeley, R., Carval, T., and The Argo Data Management Team.,2006, "Argo quality control manual," ver. 2.2, Report, 33 pp., Argo data management, 24 Nov. 2006.

[13] Fofonoff, P., and Millard Jr. R. C., 1983, "Algorithms for computation of fundamental properties of seawater," Unesco Technical Papers in Marine Science, **44**, pp. 53.

[14] Urick, R. J., 1983, Principles of Underwater Sound. McGraw-Hill, New York, pp 423.

[15] Findlater, J., 1969, "A major low-level air current near the Indian Ocean during the northern summer," Quarterly Journal Royal Meteorological Society., ***95***, pp. 362 – 380.

[16] Prasad, T. G., and Bahulayan, N.,1996, "Mixed layer depth and thermocline climatology of the Arabian Sea and western equatorial Indian Ocean," Indian Journal of Marine Sciences, ***25***, pp. 189 – 194.

[17] McCreary, J. P., Kundu, P. K., and Molinari, R. L., 1993, "A numerical investigation of dynamics, thermodynamics and mixed-layer processes in the Indian Ocean," Progress. in Oceanography, **31 (3)**, pp.181 – 244.

[18] Bauer, S., Hitchcock, G. L., and Olson, D. B., 1991, "Influence of monsoonally – forced Ekman dynamics upon surface layer depths and plankton biomass distribution in the Arabian Sea", Deep Sea Research., **38**, pp. 531 – 553.

[19] Wyrtki, K.,1973, "An equatorial jet in the Indian Ocean," Science, **181**, pp. 262 – 264.

[20] O' Brien, J. J., and Hurlburt, H. E.,1974, "Equatorial jet in the Indian Ocean: Theory. Science,", **184**, pp. 1075 – 1077.